IGARSS 2020 - 2020 IEEE International Geoscience and Remote Sensing Symposium | 978-1-7281-6374-1/20/$31.00 ©2020 IEEE | DOI: 10.1109/IGARSS39084.2020.9323556

DETECTION OF SUB-PIXEL PLASTIC ABUNDANCE ON WATER SURFACES USING AIRBORNE IMAGING SPECTROSCOPY

A. Hueni[1] and S. Bertschi[1]

[1] Remote Sensing Laboratories, University of Zurich, Winterthurerstrasse 190, 8057 Zurich, Switzerland

ABSTRACT

This work tested the practical mapping of floating plastic waste at surface area abundances between 1% - 5% using airborne imaging spectroscopy. APEX and AVIRIS-ng sensors were flown over deployed targets of known abundance during the ESA HyperSense campaign in 2018. Results show that such low abundances can be detected and mapped, while actual material identifications start to fail for abundances of 2.5% and lower.

Index Terms— *Field Spectroscopy, Airborne Spectroscopy, Ocean Plastic Waste*

1. INTRODUCTION

The pollution of the oceans and seas of the Earth is one of many environmental problems, but has recently gained a higher media and, hence, public attention. The problem manifests itself in various effects, such as entanglement of marine wildlife or ingestion leading to the potential starvation of the organism, and/or a subsequent biomagnification of toxic additives and pollutants in the food chain by the adsorption of toxic pollutants dissolved in seawater on plastic surfaces.

Various clean-up efforts have been started (e.g. www.theoceancleanup.com), but they all lack one crucial information: the actual spatial location and abundance of floating plastics. In a clean-up operation, all other phases rely on the intelligence on where to direct the operation, i.e. the Localisation phase (Figure 1). The phases of targeting, i.e. selection of areas best suited for high-yield collection, development of a mission plan (the order and manner in which that targets are to be approached) and the navigation (NAV) of vessels into the mission area all rely on spatial information about the distribution and density of the plastics. It follows naturally that the highest risk of these operations lies in the successful quantitative spatial mapping of the target material.

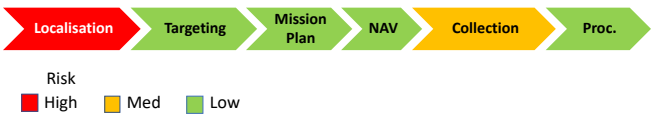

Figure 1: Operational phases of a generic ocean plastic clean-up operation

It has been claimed that remote sensing alone has the potential to map ocean waste on a global scale. Of the possible sensing technologies, imaging spectroscopy seems the most suitable [1]. This assumption is based on the use of spectroscopy to sort polymers in industrial settings. Demonstrations of spectroscopy mapping plastics floating on water surfaces from remote platforms were still sparse at the time the experiment presented in this paper was devised. This situation has recently been improved through work by e.g. Garaba et al [2].

This research aims to establish the suitability of imaging spectroscopy to map floating meso- and macro-plastics at realistic abundances on natural water bodies using the airborne imaging spectrometers AVIRIS-ng [3] and APEX [4] by imaging deployed targets of known abundance.

2. METHODS

2.1. Design of Floating Test Areas

Preliminary literature studies led to the abundances selected to be realised in artificial test areas. The often shockingly high abundances portrayed in media reports do not represent the common abundance found on the seas and oceans. More realistic figures that are still deemed detectable are in the low percentage range. Consequently, three areas were constructed, consisting of flattened PET bottles connected by strings and dimensions of 10 m x 10 m per area. The nominal abundances were 5%, 2.5% and 1% respectively.

2.2. Deployment

The test areas were deployed in three different Swiss freshwater bodies (Irchel Pond, Greifensee and Hallwilersee) and anchored to the lakebeds to keep them spatially stable. The stability was however influenced by wind and waves and the nominal abundances per area could only be met approximately.

2.3. Airborne Imaging Spectrometers

Two airborne imaging spectrometers were deployed during the 2018 HyperSense summer flight campaign organised on behalf of ESA: AVIRIS-ng operated by NASA/JPL and APEX operated by VITO and RSL.

Both sensors cover the VSWIR range of 400 nm – 2500 nm.

2.4 Data Acquisitions

APEX and AVIRIS-ng data were acquired as listed in Table 1.

Table 1: Data acquisition overview

Site	Date	Sensor	GSD [m]	AGL [m]
Greifensee	24.07.2018	APEX	2.5	5000
Hallwilersee	27.06.2018	AVIRIS-ng	4	4500
Irchel	01.07.2018	APEX	2.9	6500
Irchel	01.07.2018	AVIRIS-ng	4.1	4500

2.5 Data Preprocessing

APEX data were processed to radiances in the APEX PAF [5-7] while AVIRIS-ng data were calibrated to radiances by a dedicated processing chain at NASA/JPL [8, 9].
Atmospheric corrections were not carried out to avoid the removal of information in wavelengths dominated by water absorption, i.e. most of the spectral range [1].

2.6 Data Analysis

In an explorative approach, a number of classification and discrimination approaches were tried on the datasets, including: spectral indices, continuum removal, k-means clustering, minimum distance supervised classification, spectral angle mapper, and spectral mixture analysis. The analysis was done using a combination of ENVI modules and specifically developed Matlab code.
Only the minimum distance results are reported in this paper. While this approach is not the most appropriate for specific material identification, the results are exemplary to demonstrate the main findings of the study. To test the impact of spectral band selection or spectral space transformation on the classification result, the following sets were selected:

1. All spectral bands
2. Spectral bands according to [10]: 1667 nm, 1728 nm, and 1788 nm
3. All MNF (Minimum Noise Fraction) bands
4. Selected MNF bands, containing the most image information but omitting those bands containing mostly sensor artefact patterns
5. Absorption feature at 931 nm: 880 – 980 nm
6. Absorption feature at 1215 nm: 1100 - 1300 nm
7. Absorption feature at 1417 nm: 1400 – 1500 nm
8. Absorption feature at 1732 nm: 1650 - 1800 nm

2.7 Linear Mixing Simulation

The effects of subpixel abundances of plastics on water surfaces was investigated by carrying out a linear mixing simulation in radiance spectral space with an abundance step size of 0.5%. The water endmember consisted of an APEX mean water spectrum extracted from the Greifensee site. The PET endmember was calculated as the mean HCRF (Hemispherical-Conical Reflectance Factor) of 100% PET floating on a water surface and measured with an ASD field spectroradiometer. APEX at-sensor radiances were simulated using an ATCOR function with simulation parameters (sun angles, aerosol model, flight altitude, etc) identical to the ones used for the atmospheric correction of the APEX flight line.

3. RESULTS

A visual impression of PET densities deployed in the three test areas is given in Figure 2. This drone-based image also exemplifies the potential for confusion with sun glint due to wavelets.

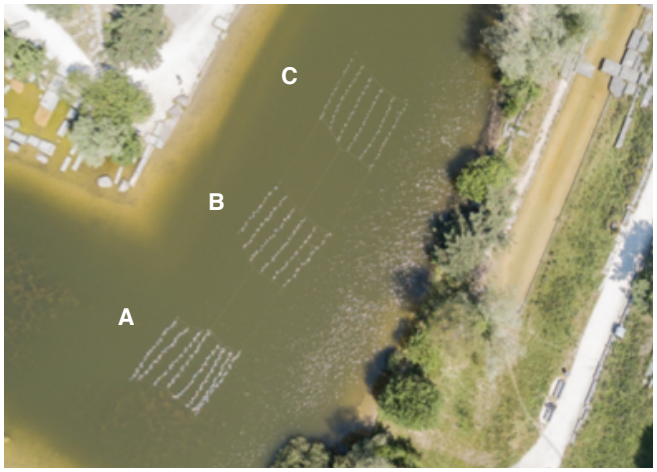

Figure 2: Test areas A (5%), B (2.5%) and C (1%) deployed on Irchel campus pond, imaged by a commercial drone camera. Sun glint due to wavelets is visible near the right-hand shore.

Mean radiance spectra of APEX and AVIRIS-ng extracted from the water surface and PET test areas show increased radiance levels that appear to scale according to the PET abundance (Figure 3). It is however obvious that no major spectral differences are discernible at these low abundances.

Classification approaches such as minimum distance have higher accuracy when restricting the spectral band range (Figure 4). Band sets in the SWIR help avoiding the confusion with bathymetry features or sensor striping artefacts.

The accuracy metrics (Figure 5) contrast overall user and producer accuracies with target area specific producer accuracies. Producer accuracies for SWIR related bands are influenced by the confusion between the different abundance classes as well by omissions due to edge effects of the finite target areas implicitly convolved by the sensor spatial response function.

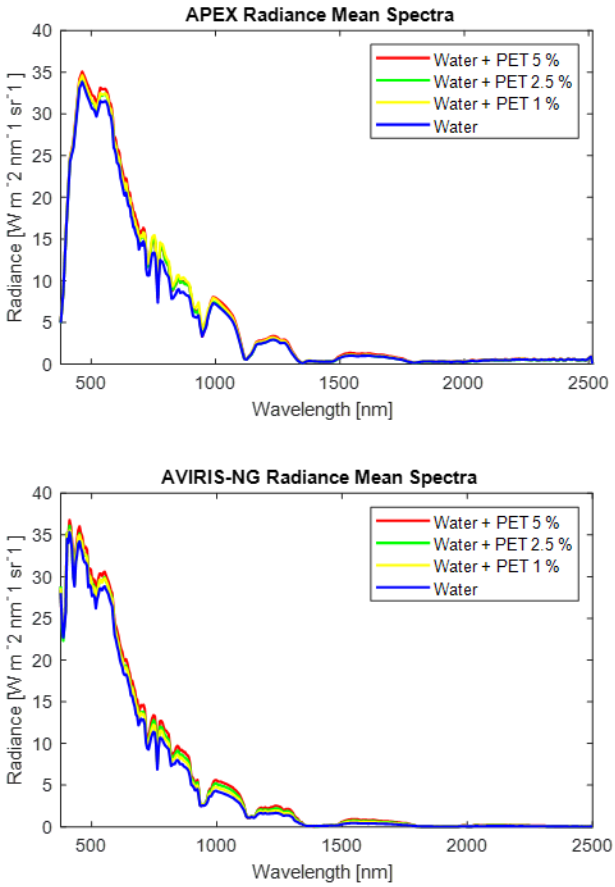

Figure 3: Average radiances of the three test areas plus water for APEX and AVIRIS-ng at the Irchel Pond site, demonstrating the small modification of the at-sensor radiance through the presence of PET material at sub-pixel abundance.

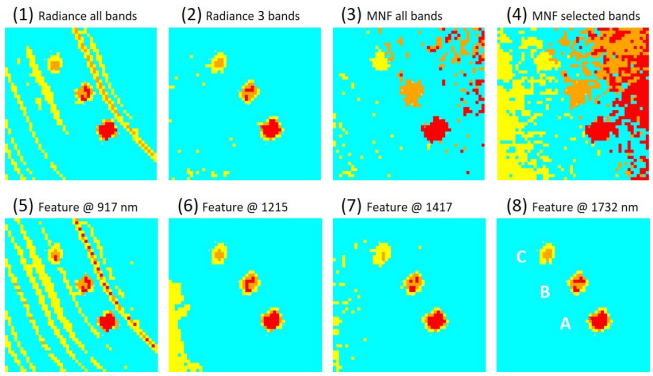

Figure 4: Results of a minimum distance supervised classification for various band sets of APEX imagery, showing the influence of bathymetry and residual striping in cases where no plastic-specific band sets in the SWIR were used. Red = 5% PET, orange = 2.5%, yellow = 1%, and cyan = pure lake water. Test areas are indicated by their alphabetic code in the lower right image.

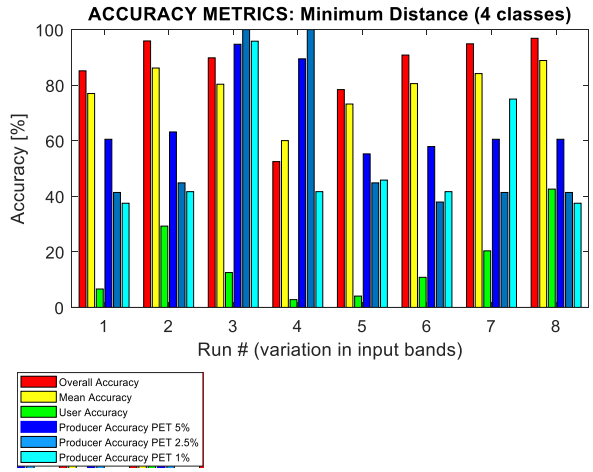

Figure 5: Accuracy metrics for the minimum distance classification

The mean water and target radiances acquired by APEX are compared to the best matching radiance spectra produced by the mixture simulation, selected by their RMSE value calculated for the range 800 – 1900 nm (Figure 6). Simulated and measured spectra and their abundances match well, despite uncertainties in atmospheric parameterisation, radiometric calibration uncertainties of APEX and uncertainties in the representativeness of the chosen PET endmember.

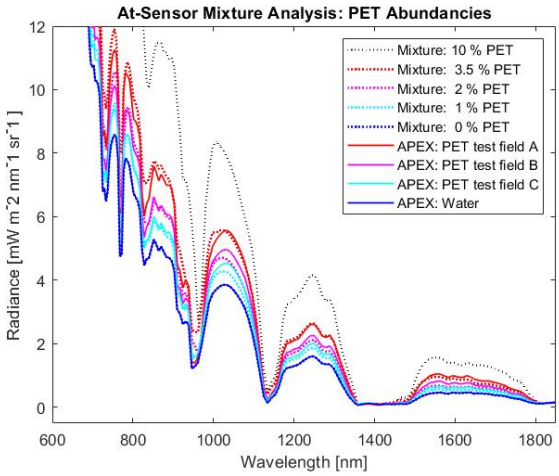

Figure 6: Comparison of mean spectral signatures extracted from APEX data with simulated spectra using linear mixing. A 10% mixture is shown for reference.

The best matching mixture for the highest abundance target underestimates the abundance by 1.5%, while 2.5% abundance target is underestimated by 0.5%. This may be attributed to the general radiometric calibration accuracy of APEX [4] but also to deviations of measurements and simulations in the water vapour absorption bands, and to values in the wavelength region affected by the APEX beam splitter (900 – 1100 nm) [7].

4. CONCLUSIONS

This study showed that PET plastic abundances in the range of 1% - 5% can be successfully discriminated and mapped under ideal circumstances using airborne imaging spectrometers at a distance of several kilometres above the water surface. The minimum distance classification results shown in this work are essentially discriminations and not material identifications per se. The main discriminator between water and plastic test area pixels lies in their radiometric intensity difference.

Material identifications require the use of unique spectral features, in this case polymer absorptions. The mean spectra extracted from APEX data in Figure 7 demonstrate the vanishing of spectral features at low abundances. The spectral bandwidth and signal to noise ratio of the sensor may play a role in how low of an abundance still results in discernible features.

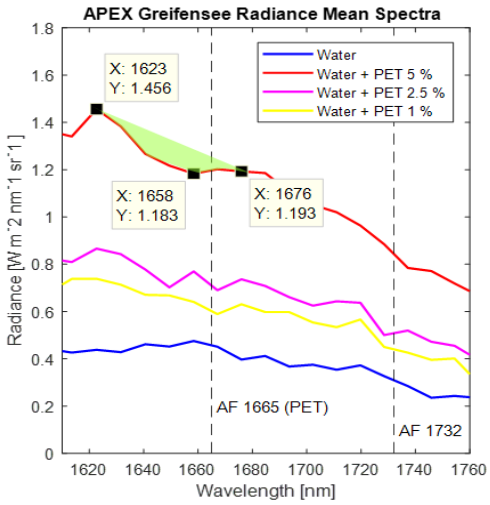

Figure 7: Mean spectra of water and the three test areas, exemplifying the vanishing of absorption features with low PET abundances for the nominal 1665 nm feature, appearing around 1660 nm due to APEX spectral shifts [7].

The linear spectral mixing approach employed in this study supports that the linear mixing assumption is valid. Consequently, further studies should employ simulation approaches to further establish the detection and hence mapping limits of imaging spectrometers under varying scenarios such as different ocean colours, wave patterns and sun glint effects.

5. REFERENCES

[1] L. Goddijn-Murphy, S. Peters, E. van Sebille, N. A. James, and S. Gibb, "Concept for a hyperspectral remote sensing algorithm for floating marine macro plastics," *Marine Pollution Bulletin,* vol. 126, pp. 255–262, 2018.

[2] S. P. Garaba, J. Aitken, B. Slat, H. M. Dierssen, L. Lebreton, O. Zielinski, and J. Reisser, "Sensing Ocean Plastics with an Airborne Hyperspectral Shortwave Infrared Imager," *Environmental science & technology,* 2018.

[3] W. J. Chapman, R. D. Thompson, C. M. Helmlinger, D. B. Bue, O. R. Green, L. M. Eastwood, S. Geier, W. Olson-Duvall, and R. S. Lundeen, "Spectral and Radiometric Calibration of the Next Generation Airborne Visible Infrared Spectrometer (AVIRIS-NG)," *Remote Sensing,* vol. 11, 2019.

[4] M. Schaepman, M. Jehle, A. Hueni, P. D'Odorico, A. Damm, J. Weyermann, F. D. Schneider, V. Laurent, C. Popp, F. C. Seidel, K. Lenhard, P. Gege, C. Küchler, J. Brazile, P. Kohler, L. D. Vos, K. Meuleman, R. Meynart, D. Schläpfer, and K. I. Itten, "Advanced radiometry measurements and Earth science applications with the Airborne Prism Experiment (APEX)," *Remote Sensing of Environment,* vol. 158, pp. 207-219, 2015.

[5] A. Hueni, J. Biesemans, K. Meuleman, F. Dell'Endice, D. Schläpfer, S. Adriaensen, S. Kempenaers, D. Odermatt, M. Kneubuehler, J. Nieke, and K. Itten, "Structure, Components and Interfaces of the Airborne Prism Experiment (APEX) Processing and Archiving Facility," *IEEE Transactions on Geoscience and Remote Sensing,* vol. 47, pp. 29-43, 2009.

[6] A. Hueni, S. Sterckx, and M. Jehle, "Operational calibration of APEX," in *2013 IEEE International Geoscience and Remote Sensing Symposium - IGARSS*, 2013, pp. 4423-4426.

[7] A. Hueni, D. Schlaepfer, M. Jehle, and M. E. Schaepman, "Impacts of Dichroic Prism Coatings on Radiometry of the Airborne Imaging Spectrometer APEX," *Appl. Opt.,* vol. 53, pp. 5344–5352, 2014.

[8] D. R. Thompson, B.-C. Gao, R. O. Green, D. A. Roberts, P. E. Dennison, and S. R. Lundeen, "Atmospheric correction for global mapping spectroscopy: ATREM advances for the HyspIRI preparatory campaign," *Remote Sensing of Environment,* vol. 167, pp. 64-77, 2015/09/15/ 2015.

[9] D. R. Thompson, J. W. Boardman, M. L. Eastwood, R. O. Green, J. M. Haag, P. Mouroulis, and B. Van Gorp, "Imaging spectrometer stray spectral response: In-flight characterization, correction, and validation," *Remote Sensing of Environment,* vol. 204, pp. 850-860, 2018/01/01/ 2018.

[10] B. Hörig, F. Kühn, F. Oschütz, and F. Lehmann, "HyMap hyperspectral remote sensing to detect hydrocarbons," *International Journal of Remote Sensing,* vol. 22, pp. 1413–1422, 2001.